Journal of Instrumentation

Tests of multigap RPCs for high-η triggers in CMS

PUBLISHED BY IOP PUBLISHING FOR SISSA MEDIALAB

RECEIVED: *July 2, 2012*
ACCEPTED: *September 12, 2012*
PUBLISHED: *October 9, 2012*

SPECIAL ISSUE ON RESISTIVE PLATE CHAMBERS AND RELATED DETECTORS RPC2012

Tests of multigap RPCs for high-η triggers in CMS

K.S. Lee,[a,1,2] **A. Aleksandrov,**[b,2] **U. Berzano,**[c,2] **C. Calabria,**[d,2] **C. Carrillo,**[e,2] **A. Colaleo,**[d,2] **V. Genchev,**[b,2] **P. Iaydjiev,**[b,2] **Y.G. Jeng,**[a,2] **M. Kang,**[a,2] **F. Loddo,**[d,2] **M. Maggi,**[d,2] **S.K. Park,**[a,2] **G. Pugliese,**[d,2] **M. Rodozov,**[b,2] **S.S. Shin,**[a,2] **M. Shopova,**[b,2] **K.S. Sim,**[a,2] **G. Sultanov**[b,2] **and P. Verwilligen**[f,2]

[a] *Department of Physics and Korea Detector Laboratory, Korea University, Anam-dong 5-ga, Sungbukgu, Seoul, Republic of Korea*
[b] *Bulgarian Academy of Sciences, Institute for Nuclear Research and Nuclear Energy, Tzarigradsko shaussee Boulevard 72, 1784, Sofia, Bulgaria*
[c] *Università degli Studi di Pavia and INFN — Sezione di Pavia, Via Bassi 6, Pavia, Italy*
[d] *Università degli Studi di Bari and INFN — Sezione di Bari, Via Orabona 4, 70126, Bari, Italy*
[e] *Università degli Studi di Napoli and INFN — Sezione di Napoli, Complesso Univ. Monte S. Angelo, Via Cintia, 80126, Napoli, Italy*
[f] *Department of Physics, Ghent University, Proeftuinstraat 86, 9000, Ghent, Belgium*

E-mail: kslee0421@korea.ac.kr

ABSTRACT: In this paper, we report a systematic study of multigap Resistive Plate Chambers (RPCs) for high-η triggers in CMS. Prototype RPC modules with four- and six-gap structures have been constructed with phenolic high-pressure-laminated (HPL) plates and tested with cosmic muons and gamma rays irradiated from a 200-mCi ^{137}Cs source. The detector characteristics of the prototype multigap RPCs were compared with those of the double-gap RPCs currently used in the CMS experiment at LHC. The mean values for detector charges of cosmic-muon signals drawn in the four- and six-gap RPCs for the efficiency values in the middle of the plateau were about 1.5 and 0.9 pC, respectively, when digitized with charge thresholds of 150 and 100 fC, respectively. They were respectively about one third and one fifth of that drawn in the current CMS double-gap RPC with a charge threshold of 200 fC. We concluded from the current R&D that use of the current phenolic-HPL multigap RPCs is advantageous to the high-η triggers in CMS in virtue of the smaller detector pulses.

KEYWORDS: Gaseous detectors; Particle tracking detectors (Gaseous detectors)

[1] Corresponding author.
[2] On behalf of the CMS collaboration.

doi:10.1088/1748-0221/7/10/P10009

Contents

2012 JINST 7 P10009

1 Introduction

The Compact Muon Solenoid (CMS) has been constructed at the European Center for Nuclear Research (CERN) to explore Higgs and Supersymetric particles and to address new physics in general using the Large-Hadron-Collider (LHC) beams. In CMS, Resistive Plate Chambers (RPCs) play an important role in the efficient detection of muon signals [1, 2].

The required detection rate capability of the present CMS double-gap RPCs to perform muon triggers in the LHC collision runs with a designed maximum luminosity of 10^{34} cm^{-2}s^{-1} is 1 kHz cm^{-2} [2]. However, the maximum background rate in the CMS RPCs in the highest η region would exceed 1 kHz cm^{-2} when the luminosity increases to a level of 10^{35} cm^{-2} s^{-1} in future.

During the last decades, gas mixtures composed of tetrafluoroethane ($C_2H_2F_4$, R134a Freon) and isobutane ($i\,C_4H_{10}$) have been widely used for the operation of the phenolic-HPL trigger RPCs. A relatively large gain of the ionization avalanche and stability with a wide operational plateau have been the advantages of the use of the Freon-based gas mixtures. However, the large detector pulses would be a drawback when the particle rate is high. The detector current drawn in a double-gap RPC with a typical size of 2 m^2 will far exceed the practical limit of the RPC operation ($\sim$ 1 mA) when the particle rate reaches a few kHz cm^{-2} [3]. Furthermore, it was found from past aging studies [4] that the degradation of the detector performance due to Freon radicals contained in the detector gas [5] was dramatically accelerated when the background particle rate exceeded 3 kHz cm^{-2}.

Size reduction of the avalanche signals drawn in the trigger RPCs, therefore, lessens the probability of degradation due to the high-rate beam background. Here, we propose a development of multigap RPCs whose detector pulses and the particle-induced currents are significantly smaller than those drawn in the present CMS double-gap RPCs.

In this paper, details for prototype four- and six-gap RPCs are described in section 2. The electronics setup to examine the prototype multigap RPCs with cosmic muons and gamma rays emitted from a 200-mCi ^{137}Cs gamma-ray source is briefly explained in section 3. In section 4, the detector characteristics of the multigap RPCs obtained in the tests are compared with those of the current double-gap RPCs. Finally, the conclusions for the phenolic multigap RPCs developed in the present R&D are summarized in section 5.

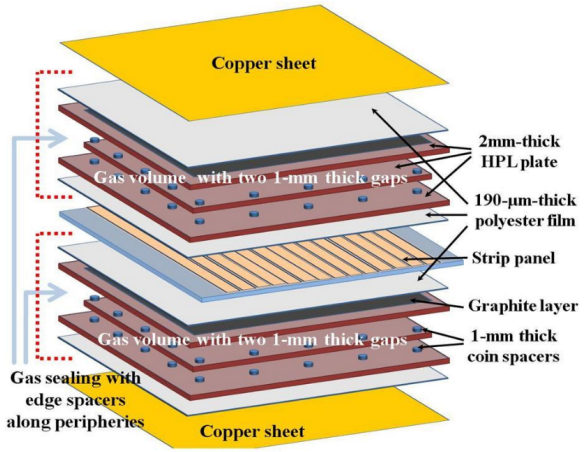

Figure 1. Schematic diagram for a 1 mm-thick four-gap RPC

2 Description of multigap RPCs

Phenolic high-pressure-laminated (HPL) was the basic resistive-plate material for the multigap RPCs developed in the present study, while thin glass is typically used for timing RPCs [6, 7]. In the present research, prototypes detectors with four- and six-gap structures have been constructed for a systematic study of detector charges and the responses to intense gamma-ray background.

As illustrated in figure 1, a four-gap RPC was composed of two separated 1 mm-thick double-layer gas volumes. In a similar way, a six-gap RPC was composed of two separated 0.66 mm-thick triple-gap gas volumes. The HPL plate(s) placed in the middle of each gas volume were automatically biased at an intermediate potential(s) when an electrical potential is applied to the graphite electrode coated on the two outmost HPL plates. The mean values of the bulk resistivities for the 2- and 1 mm thick HPL sheets measured at $T = 20°$C were 0.95 and $6.9 \times 10^{10}\,\Omega\cdot$ cm, respectively.

The thicknesses of the circular spacers to support the gap thickness for the four- and sixgap RPCs were 1.0 and 0.66 mm, respectively. The thickness of the HPL plates used for the four and six-gap RPCs was 2 and 1 mm, respectively. Copper strips were attached on a 190 μm thick polyethylene film, and were placed between the two gas volumes for signal readouts. The pitches of the strips for the four- and the six-gap RPCs were 27 and 20 mm, respectively.

3 Experimental setup

The electronics setup to test the prototype multigap RPCs was optimized for precision measurements of detector charges for muon and gamma-ray signals, and the gamma-induced currents drawn in the detectors. As shown in figure 2, the signals induced in the RPC strips were linearly amplified by a factor of 10 by using a linear amplifier (CAEN N412). One of the amplifier outputs of each channel was discriminated by applying a proper voltage-sensitive threshold for the RPC raw pulses, and was fed into a time-to-digital converter (TDC, LeCroy 2228) after being properly delayed to satisfy a common-start-mode acquisition. The other amplifier output was also properly delayed and fed into an analog-to-digital converter (ADC, LeCroy 2249) to perform the charge measurements. The voltage thresholds applied to digitize the four and six-gap RPC pulses were 1.3 and 1.0 mV,

2012 JINST 7 P10009

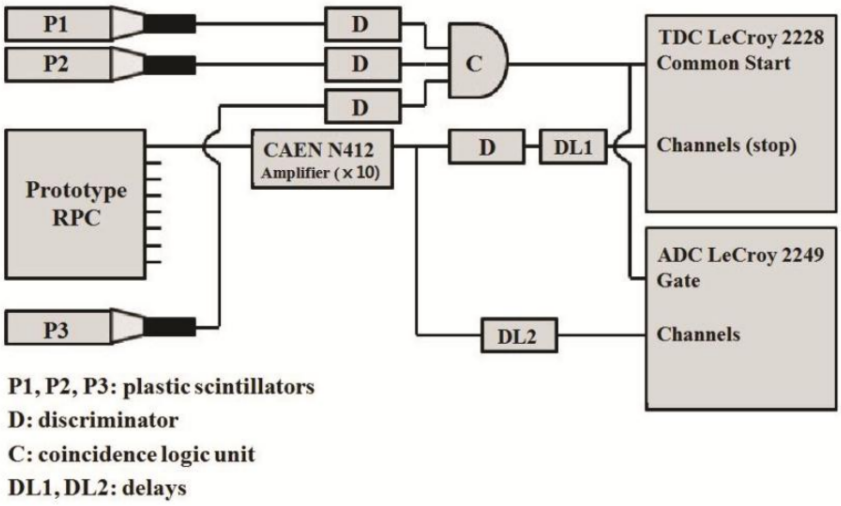

Figure 2. Schematic diagram of the electronics setup for tests with cosmic muons and gamma rays.

respectively, which were estimated to be approximately equivalent to charge thresholds of 150 and 100 fC, respectively, from the offline data analysis.

Cosmic muons were triggered by a triple coincidence of plastic scintillators equipped with photomultipliers (Hamamatsu model H2431). The scintillator signals were digitized with a 30 mV voltage threshold, and were fed into the TDC Start and the ADC Gate. Data for noises and gamma rays were obtained by 1 kHz clock triggers provided by using a 2 GHz pulse generator. The rates of the noises and gamma-ray signals induced in unit areas of the detectors were properly estimated from the numbers of hits occurring in the time periods allowed by the clock triggers.

The prototype multigap RPCs were examined in avalanche mode using a gas mixture of 95.7% $C_2H_2F_4$, 3.5% $i\,C_4H_{10}$, 0.5% SF_6, and 0.3% water vapour in mass ratio. The ratio of SF_6, 0.5%, was the minimum reliable value provided by the gas system used in the current tests. The standard gas mixture for double-gap RPCs in the current CMS operation is composed of 96.2% $C_2H_2F_4$, 4.2% $i\,C_4H_{10}$, and 0.3% SF_6. However, we expect that the small discrepancy in the gas mixtures does not significantly affect to the results required to understand the fundamental differences among double-gap and multigap RPCs.

In order to draw consistent test results, applied high-voltage (HV_{app}) values were converted to effective values (HV_{eff}) under the standard conditions, $P = 1013$ hPa and $T = 293$ K [8]. The prototype multigap RPCs were installed at a mean distance of 45 cm from a 200 mCi ^{137}Cs gamma source to examine detector responses to high-rate gamma rays. The actual activity of the 10-year old gamma source was expected to be about 150 mCi (5.5 GBq).

4 Results

Figures 3 shows efficiencies (ε, full circles) and mean charges ($\langle q_e \rangle$, open circles) for muon signals, as functions of HV_{eff}, measured by the four- (left) and six-gap (right) RPCs. Muon hits having streamer pulses ($\langle q_e \rangle \geq 10$ pC) were not included in the calculation of the mean charges in figure 3.

2012 JINST 7 P10009

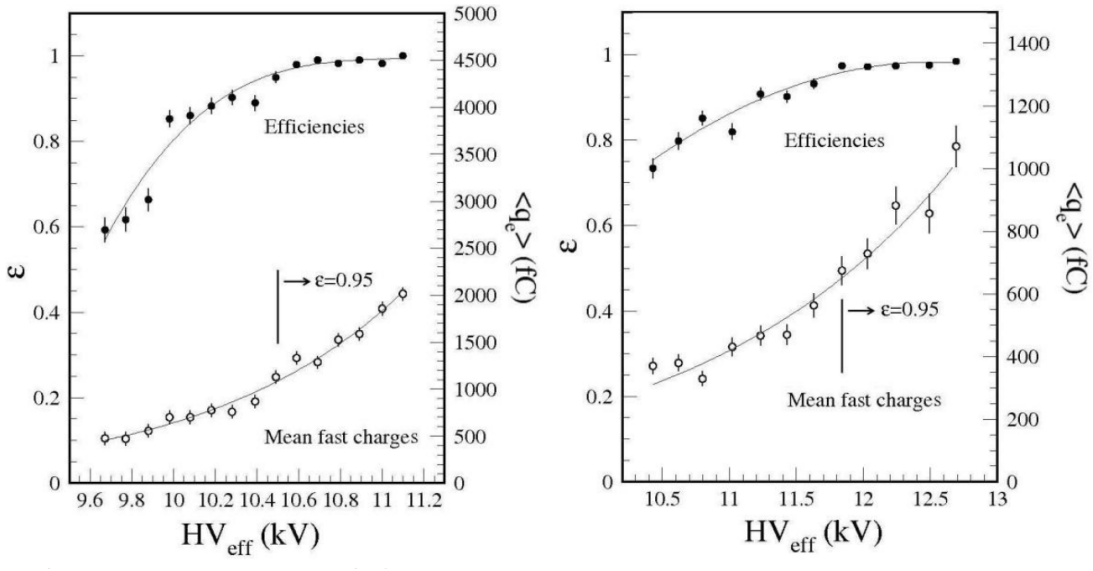

Figure 3. Efficiencies (ε, full circles) and mean charges ($\langle q_e \rangle$, open circles) of muon signals, as functions of HV_{eff}, measured by four- (left) and six-gap (right) RPCs. The solid lines in both figures were drawn to guide the trends of data.

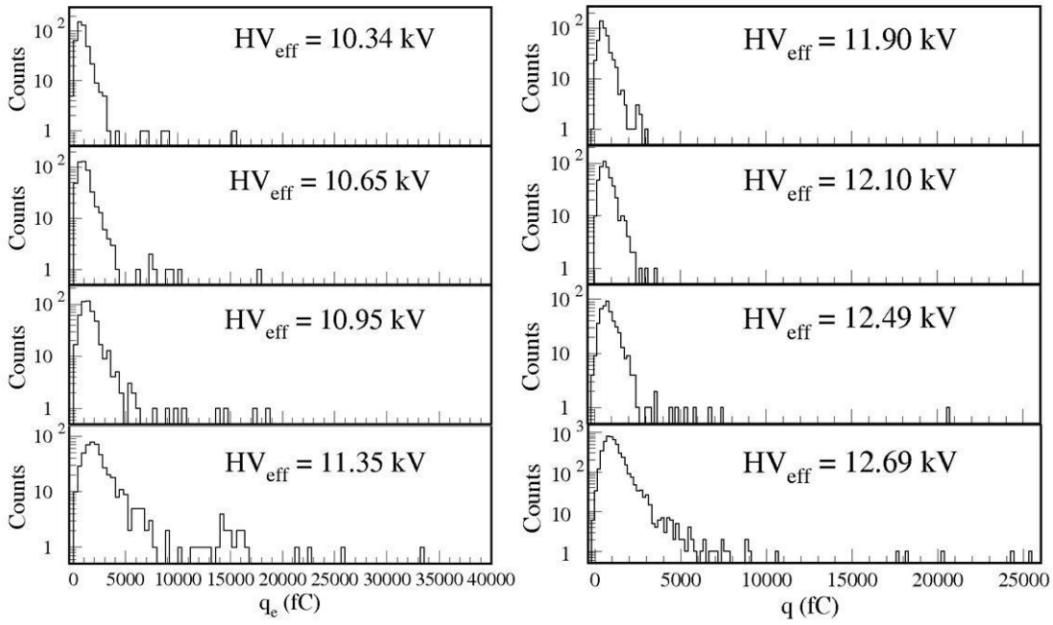

Figure 4. Charge distributions of muon signals measured by four- (left) and six-gap (right) RPCs at four different HV_{eff}'s.

As shown in figure 3, the mean charges of the muon signals drawn in the four- and sixgap RPCs, measured at the efficiency values in the middle of the plateau, were 1.5 and 0.9 pC, respectively. They were respectively about one third and one fifth of that drawn in a typical 2 mm-thick double-gap RPC when measured with a threshold of 200 fC [9].

2012 JINST 7 P10009

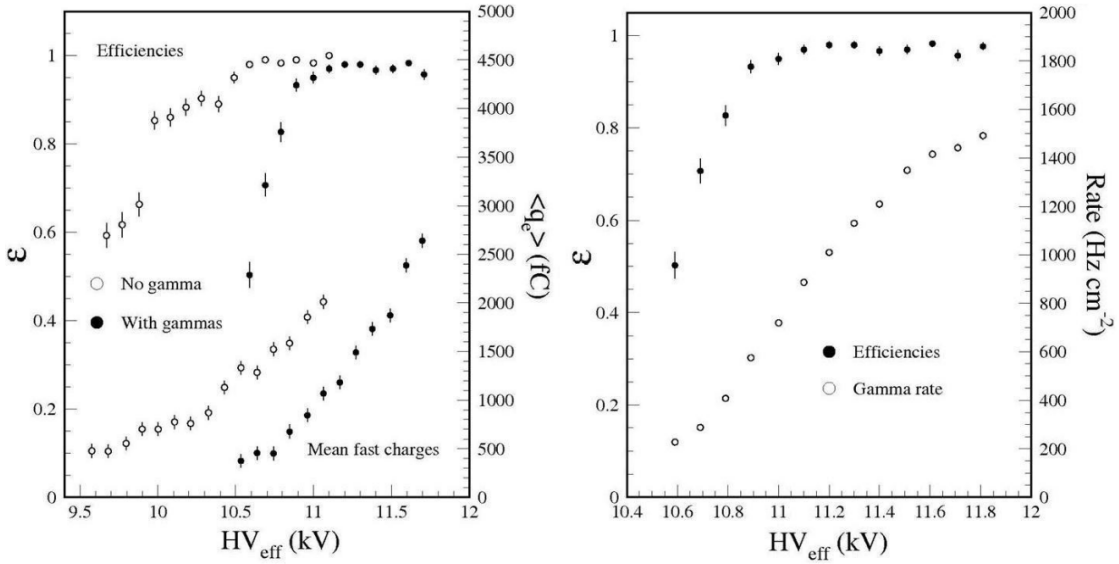

Figure 5. Left: efficiencies (ε) and mean charges ($\langle q \rangle$) of muon signals as functions of HV_{eff}, measured by a four-gap RPC, with (open circles) and without the presence of gamma background hits (full circles). Right: gamma-signal rates measured as a function of the HV_{eff}.

Comparison of charge distributions of muon signals drawn in double-, four-, and six-gap RPCs allows us to envisage their different scopes in the usable ranges of the avalanche-mode pulses. Figure 4 shows the charge distributions drawn in the four- (left) and six-gap (right) RPCs at four different HV_{eff}'s. As figure 4 shows, the upper limits of the avalanche pulses for the four- and six-gap RPCs were about 10 and 6 pC, respectively, while it extended to 25 pC for the double-gap RPCs [9]. Considering the charge distributions and the upper limits of the avalanche pulses, the choices of the threshold values of 150 and 100 fC, respectively, for the four- and sixgap RPCs were expected to be relevant. We also expect that lowering the thresholds below the chosen values would make the detectors more sensitive to gamma-ray signals with smaller charges.

As shown in figure 4, the streamer probabilities ($\langle q_e \rangle \geq 10$ pC) measured at their maximum HV_{eff}'s for the four (bottom left) and six-gap RPCs (bottom right) were 0.09 and 0.03, respectively. Therefore, we conclude that the sizes of the muon efficiency plateaus for both detectors, measured with the current electronics setup, were larger than 600 V.

The left part of figure 5 shows efficiencies (ε) and mean charges ($\langle q_e \rangle$) of the muon signals, measured by the four-gap RPC, as functions of HV_{eff}, with (open circles) and without the presence of gamma-background hits (full circles). The right part of figure 5 shows the gammasignal rates also measured as a function of the HV_{eff}. The measured rates of gamma rays appeared in the muon efficiency plateau ranged from 0.7 to 1.5 kHz cm^{-2}. The shift of the efficiencies and the mean charges in the HV_{eff} due to the gamma-signal rate of ~ 1 kHz cm^{-2} was about 400 V, which was comparably smaller than the size of the muon efficiency plateau.

The charge distributions for the muon (left) and gamma-ray signals (right) measured by the four-gap RPC at two HV_{eff}'s laid in the muon efficiency plateau are shown in figure 6. The charge distributions in both-side panels in figure 6 were obtained with presence of the same gamma-ray flux. The gamma-signal rates at $HV_{eff} = 11.1$ and 11.3 kV were 0.90 and 1.14 kHz cm^{-2} respectively. Recalling the difference between the charge distributions of the muon and gammaray

2012 JINST 7 P10009

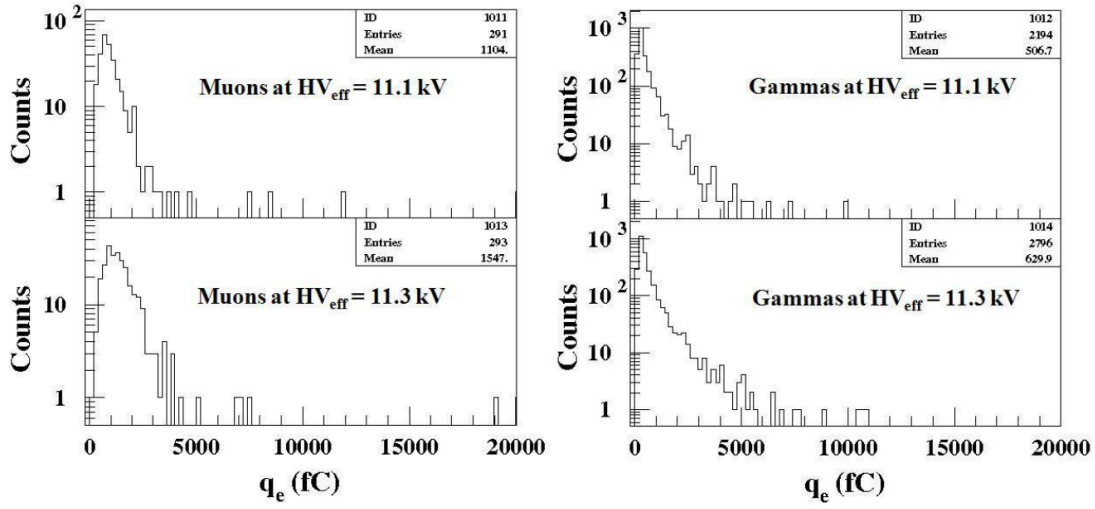

Figure 6. The charge distributions of muon (left) and gamma-ray signals (right) measured by a four-gap RPC at two HV_{eff}'s in the muon efficiency plateau. The charge distributions in both-side panels were obtained with presence of the same gamma-ray flux.

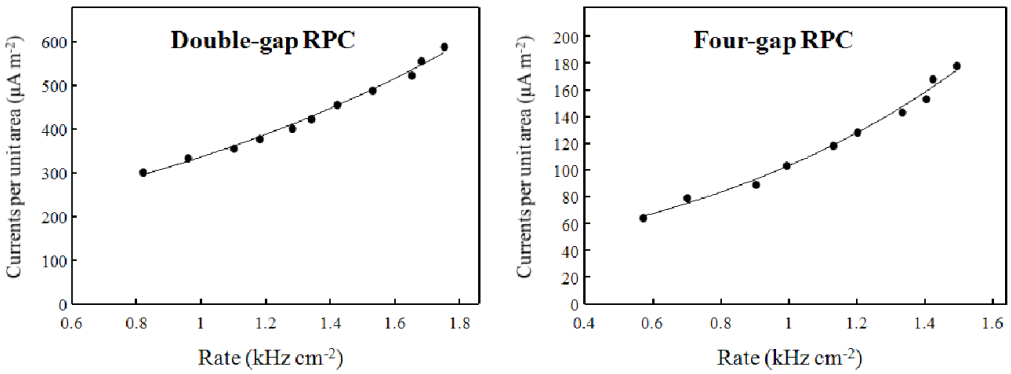

Figure 7. Gamma-ray induced currents drawn in unit areas of double-gap (left) and four-gap (right) RPCs as functions of the gamma-signal rate. The solid lines drawn in both figures were only to guide the trends of data.

signals, a further systematic study will be required to optimize the digitization threshold so as to make the detectors less sensitive to neutral background particles, such as gamma rays and neutrons.

Figure 7 shows gamma-induced currents drawn in unit areas of double-gap (left) and fourgap (right) RPCs as functions of the gamma-signal rate. The charge threshold to digitize the gamma-ray signals drawn in the double-gap RPC was set to 200 fC [10]. We conclude from figure 7 that the detector current induced by gamma-background hits could be reduced by a factor three when the four-gap detector configuration is adopted instead of the current double-gap one for the CMS trigger RPCs.

5 Conclusions

The goal of the present R&D was to improve detection performances of panel-type trigger RPCs constructed with phenolic HPL when they are to be operated in an environment of high

2012 JINST 7 P10009

particle-background rate exceeding 1 kHz cm^{-2}. We drew the following conclusions from the present research:

(1) The mean charges drawn in the four- and six-gap RPCs measured for the efficiency values in the middle of the plateau were about 1.5 and 0.9 pC, respectively, when digitized with charge thresholds of 150 and 100 fC, respectively. They were respectively about one third and one fifth of that drawn in a double-gap RPC with the charge threshold of 200 fC. The size reduction of the avalanche signals is fairly conductive to lessen the probability of degradation of detector due to the high-rate beam background.

(2) The usable sizes of the muon efficiency plateaus for the four- and six-gap RPCs were at least 600 V, which were relatively wider than that for the current CMS double-gap RPC ($\sim$ 400 V) operated with the approximately same gas mixture. We expect that the wider efficiency plateau is conductive to obtain more reliable operational conditions for the maintenance of detectors.

A systematic study on the digitization thresholds is required to find optimal conditions for the muon detection while allowing minimal sensitivities to the gamma-ray and neutron background particles. Furthermore, development of real-size detector modules is essential to optimization of the detector structure for the CMS RPC trigger system.

Acknowledgments

This work was supported by a Korea University Grant (research fellow program) and by the National Research Foundation of Korea under grant numbers K20802011718-11B1301-00610 (for Korean CMS researches) and 2012029403 (for nuclear science researches).

References

[1] CMS collaboration, *Detector performance and software – Technical design report volume I*, CERN-LHCC-2006-001 (2006).

[2] CMS collaboration, *The Muon project, technical design report*, CERN-LHCC-97-032 (1997).

[3] H.C. Kim et al., *Aging study with high-level radiation sources for the CMS forward RPCs*, *J. Korean Phys. Soc.* **52** (2008) 913.

[4] H.C. Kim et al., *Quantitative aging study with intense irradiation tests for the CMS forward RPCs*, *Nucl. Instrum. Meth.* **A 602** (2009) 771.

[5] M. Abbrescia et al., *HF production in CMS-Resistive Plate Chambers*, *Nucl. Phys. (Proc. Suppl.)* **B 158** (2006) 30;
G. Aielli et al., *Fluoride production in RPCs operated with F-compound gases*, *Nucl. Phys. (Proc. Suppl.)* **B 158** (2006) 143.

[6] Ph. Rosnet, *The ALICE muon trigger system: cosmic ray commissioning and first beam-induced events*, *Nucl. Instrum. Meth.* **A 617** (2010) 362;
M.C.S. Williams, *The multigap RPC: the time-of-flight detector for the ALICE experiment*, *Nucl. Instrum. Meth.* **A 478** (2002) 183.

2012 JINST 7 P10009

[7] I. Deppner et al., *The CBM time-of-flight wall*, *Nucl. Instrum. Meth.* **A 661** (2012) S121;
A. Akindinov et al., *RPC with low-resistive phosphate glass electrodes as a candidate for the CBM TOF*, *Nucl. Instrum. Meth.* **A 572** (2007) 676.

[8] M. Abbrescia et al., *Study of long-term performance of CMS RPC under irradiation at the CERN GIF*, *Nucl. Instrum. Meth.* **A 533** (2004) 102.

[9] S.H. Ahn et al., *Characteristics of a double gap resistive plate chamber for the endcap region of CMS/LHC: data vs. simulation in avalanche mode*, *Nucl. Instrum. Meth.* **A 533** (2004) 32;
Performance and simulation of a double-gap resistive plate chamber in the avalanche mode, *J. Korean Phys. Soc.* **45** (2004) 1490.

[10] S.H. Ahn et al., *Systematic studies of aging effects in RPCs for the CMS/LHC experiment*, *J. Korean Phys. Soc.* **47** (2005) 427.

2012 JINST 7 P10009